Civil Engineering Infrastructures Journal xx,xx
DOI: 10.22059/CEIJ.2023.351287.1889

Optimization of Dynamic Compaction Procedure for Sandy Soils

Meysam Bayat[1], Mohsen Saadat[1,*], Arghavan Hojati[2]

1- Assistant Professor, Department of Civil Engineering, Najafabad Branch, Islamic Azad University, Najafabad, Iran

2- MSc Graduated, Department of Civil Engineering, Najafabad Branch, Islamic Azad University, Najafabad, Iran

Corresponding author: mohsen.saadat@pci.iaun.ac.ir, ORCID : 0000-0001-9505-4893

Received: 18/11/2022
Revised: 18/06/2023
Accepted: 03/07/2023

Abstract

Dynamic Compaction (DC) is employed as a simple and economical method to improve weak soils in the last few decades. DC is usually applied for granular soils by falling a heavyweight (up to 40 tons) from a height (up to 40 meters) at regularly spaced intervals. Significant issues in DC are the weight and height of the tamper, compaction pattern and the distance between tamping locations. Incorporated innovation in this paper is to introduce an analytical approach to optimize the compaction pattern and DC variables regarding regular constraints. The required energy for compaction is evaluated for square and diamond patterns. DC optimization is a non-linear and non-convex problem due to nonlinear equations in soil compaction behavior. Thus, a metaheuristic approach (Genetic Algorithm) is employed to find global optimum. The optimum answer presents the minimum compaction energy in each pattern. Results indicated that the maximum allowed values of tamper mass and the number of tamper drops were required to minimize

compaction energy. The ratio of compaction energy at diamond pattern to square one was also found to be about 0.75 to 0.90 for the same compaction conditions.

***Keywords*:** Dynamic Compaction, Ground Improvement, Sandy Soils, Optimization

Introduction

Soil improvement techniques improve the engineering properties of soli, like strength, stiffness, and permeability (Anand and Sarkar, 2021; Ghanbari and Bayat, 2022; Sahlabadi et al., 2021; Haghbin and Ghazavi, 2016; Salehi et al., 2021). Soil compaction is widely used in geotechnical projects to reduce the foundation and construction and/or any unexpected risks. During civil projects, geometrical compaction is essential in reducing the inter-granular porosity to reach a high relative density (Ghassemi and Shahebrahimi, 2020; Mehdipour and Hamidi, 2017; Paranthaman and Azam, 2022; Raja and Thyagaraj, 2020; Silveira and Rodrigues, 2020). Dynamic Compaction (DC) is a relatively traditional and old-fashioned method introduced by Menard and Broise in the early 1970s and was applied to improve the granular soils only (Ménard and Broise, 1975). The DC technique is a type of ground improvement method that involves the repeated high-energy impacts to the soil surface using a heavyweight (up to 40 tons) with drop heights from 10m to 40m. Previous studies reveal that DC technique could be widely used to stabilize loose granular materials and waste landfills to its ease of implementation, economically competitive and environmentally safe (Gu and Lee, 2002). Obtaining soil improvement in quantitative engineering units during the DC has been a challenge with various techniques used in previous studies (Adam et al., 2007). Feng et al. (2000) used a conical-based pounder to improve the efficiency of DC. The results of laboratory DC tests showed that the efficiency of the used DC method depends on both the grain size distribution and the volumetric response of the sand. The same results have been reported for a conical pounder by Arslan et al. (2009). Hu et al. (2001) studied the effect of DC on the shear strength characteristics of loess. The experimental results revealed that the shear strength of loess increased with the number of drops and after a peak value, the shear strength decreased. Shen et al. (2018) studied the influence of DC on liquefaction potential of silty sand. The effect of DC on liquefaction potential was evaluated using CPTs before and after DC. There is nowadays a renewed interest in DC due to its advantages over other types of soil improvement techniques (Feng et al., 2010; Feng et al., 2015; Ghassemi et al., 2010; Li et al., 2011; Wang et al., 2013; Zhang et al., 2019).

Feng et al. (2017) presented a method of modeling preloading consolidation with drains and dynamic compaction in a centrifuge using a 3D printing technique. This method performed well in predicting the surface settlement, excess pore pressure and effective pressure, number of drops, and improvement depth by DC. So far, several models have been introduced for DC technique in the previous studies which were developed primarily based on several in situ experiences and physical modeling tests (An et al., 2020; Chen et al., 2019). However, previous studies mainly focused on the research of single-location tamping but the influence of adjacent tamping locations and the multi-location tamping has not been widely considered (Feng et al., 2010; Feng et al., 2013; Ménard and Broise, 1975; Wang et al., 2013). Experimental studies of multi-location tamping consider the interaction between the adjacent tamping locations, which helps understand the soil behavior in response to the impact of tampers during DC procedure.

The effective depth of DC or the depth of improvement as the affected depth during compaction is a key parameter for designing the DC procedure. The improvement depth was usually predicted using empirical correlations in the practical design procedure (Scott et al., 2021). Ménard and Broise (1975) proposed Equation (1) to estimate the improvement depth based on the energy per drop where n is an influential factor in the sense of depth of improvement. This equation was modified later by other researchers.

$$Z = n\sqrt{MH} \tag{1}$$

Over the last several years, there have been quite extensive studies to identify appropriate values of n, ranging from 0.3 to 1 depending soil types (Mostafa and Liang, 2011). Zou et al. (2008) proposed an equation to estimate Z depending on the tamper mass and area, the falling height, the number of tamper drops, the dry unit weight and water content of soil. Oshima and Takada (1999) conducted a series of centrifuge tests to analyze Z values. Based on the results of centrifuge tests, Z was considered as the depth at which the relative density (D_r) of the soil increases by more than 5%. Oshima and Takada (1999) carried out a series of geotechnical centrifuge tests to evaluate the compacted areas of multi-location tamping. Based on the test results, the soil-improvement zone with depth Z and radius R was defined according to Figure 1.

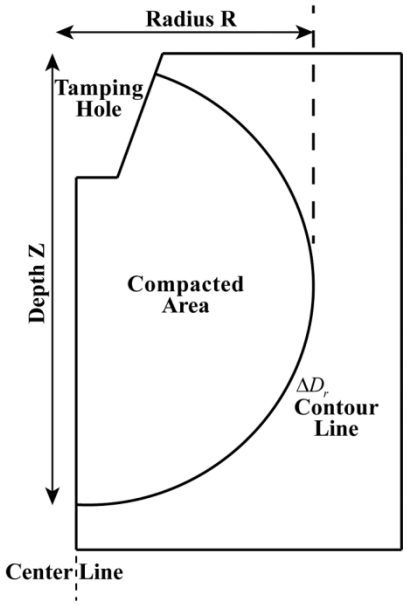

Figure 1. Dimensions of the soil-improvement zone (Oshima and Takada, 1999)

The depth and radius of the soil-improvement zone were described by the Equations (2) and (3) proposed by Oshima and Takada (1999);

$$Z = a_z + b_z \log(M \times \sqrt{2gH} \times N) = a_z + 0.434 b_z \ln(M \times \sqrt{2gH} \times N) \quad (2)$$

$$R = a_R + b_R \log(M \times \sqrt{2gH} \times N) = a_R + 0.434 b_R \ln(M \times \sqrt{2gH} \times N) \quad (3)$$

Earlier studies mainly focused on the test results such as shear wave velocity measurement (V_s), standard penetration test (SPT), and cone penetration test (CPT) before and after DC which were applied widely in the site investigation (Du et al., 2019; Feng et al., 2010; Ménard and Broise, 1975). For example, Chow et al. (1992) studied the effect of print spacing (distance between tamper locations) on the degree of improvement in DC. Based on the results, an approach to estimate the improvement radius of the soil-improvement zone was presented based on assessing the degree of improvement by the increase in friction angle of granular soils. The estimation of the friction angle was derived from indirect empirical correlation with CPT measurement.

Optimization techniques in civil engineering for reducing the time and cost of projects have attracted the interest of many researchers worldwide (Bağrıaçık et al., 2020; Biabani et al., 2022; Fazli, 2022; Hosseini et al., 2022; Kalantary and Kahani, 2019; Kaveh and Zaerreza, 2022). In recent years, many studies have been conducted on optimizing dynamic compaction design using various methods such as fuzzy logic and

artificial intelligence (Pasdarpour et al., 2009; Wang et al., 2003). In the field of optimization approaches, the Genetic Algorithm (GA) is a well-known optimization method initiated by Holland (1992) and developed by Goldberg (1989). As a member of the family of metaheuristic algorithms, GA is constructed based on the Darwinian evolution theory. It is appropriate especially for non-convex and non-linear optimization problems, where traditional gradient-based algorithms do not have a satisfactory performance to find global optimum. Details of GA procedure may be found in many literature and thus are not described here (Holland, 1992). Pasdarpour et al. (2009) presented a fuzzy-GA methodology for the optimal design of soil dynamic compaction. The results indicated that the GA produced the optimal design of soil dynamic compaction. An et al. (2020) studied the optimization of DC design to minimize the remaining compaction time using a Compaction Process-Dynamic Optimization Method (CPDOM) based on the GA. The results proved that CPDOM may be employed for civil engineering projects. Wang and Yin (2020) presented a model to predict the soil compaction parameters using multi- expression programming (MEP). The validity analyses of the model indicated that the proposed model could be used for various soil types with high accuracy.

Wang et al. (2013) based on the experimental results indicated that DC frequency was an important parameter in soil densification. Wu et al. (2020) carried out a large-scale field test to study vibration velocities from dynamic compaction of granular soil. The results indicated that the soil-improvement zone was roughly cylindrical with the same diameter as the tamper, located immediately beneath the tamper.
As mentioned, DC has been studied a lot during the past decades. However, this study aims to introduce an innovative approach to optimize the pattern and design variables incorporated in DC. Required relations for the simulation of DC were employed based on the proposition of Oshima and Takada (1999) according to Equations (2) and (3). The optimization problem consists of minimizing the required energy for DC by properly selecting patterns and related variables since certain practical constraints must be satisfied.

Materials and Methods

Proper simulation of soil compaction is essential to optimize the pattern and related variables of DC. Proposed equations by Oshima and Takada (1999) were employed in this study. The equations were presented to determine both of the depth and radius of the compacted zone. The compacted bubbles inside the soil were estimated for any combination of tamper mass, drop height and the number of drops. Proper

choosing of the pattern and distances between tamping locations is needed for efficient and economical DC operation.

The intersection of adjacent compaction bubbles is presented in Figure 2 to consider the compacted zone between two adjacent tamping locations. This study assumes that the compaction characteristics at all tamping locations are the same. The intersection of two bubbles is taken place in the depths equal to *Z′* and *Z″* according to Figure 2, where the common zone between bubbles has enough compaction. As shown by Figure 2, *Z′* and *Z″* are the distance of the ground surface from the intersection point of the two bubbles at the bottom and upside of the bubbles, respectively. Evidently, the depths of *Z′* and *Z″* depend on the horizontal distance between tamping locations (*KR)*. These depths may be determined in terms of *KR*, where *K* is a coefficient between 1 and 2 theoretically and *R* is introduced in the previous section. The values below about 1.2 for *K* is not economical while *"K=2"* means two adjacent compaction bubbles are tangent to each other.

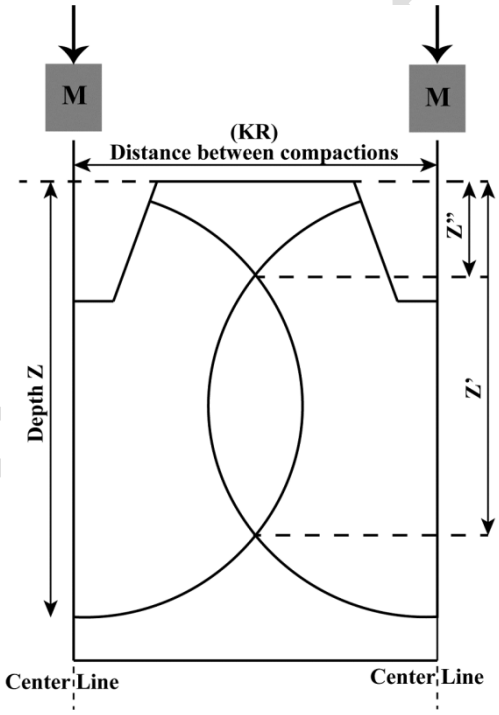

Figure 2. Intersection of adjacent compaction bubbles with distance *KR*

Intersection points on the boundary of bubbles were employed to estimate the values of *Z′* and *Z″* in terms of *KR*. For this purpose, 15 different values were chosen for *K* between 1.2 and 2 and the adjacent bubbles were drawn for each case. The values of *Z′* and *Z″* were measured for each value of *K* and, as a result, 15 pairs of (K, Z') and (K, Z'') were obtained. After eliminating *R* in relations among *KR*, *Z′* and *Z″*, the equations are estimated by fitting a quadratic function on the results. Finally, the relation of *K′* and *K″*

versus of *K* were calculated by Equations (4) and (5), respectively. These equations are required during the optimization procedure.

$$K' = -1.47K^2 + 4.14K - 1.35 \quad where \quad Z' = K' \times R \tag{4}$$

$$K'' = 1.54K^2 - 4.33K + 3.55 \quad where \quad Z'' = K'' \times R \tag{5}$$

Another issue during DC is the compaction pattern. Generally, two patterns of square and diamond were employed in this study according to Figures 3 and 4.

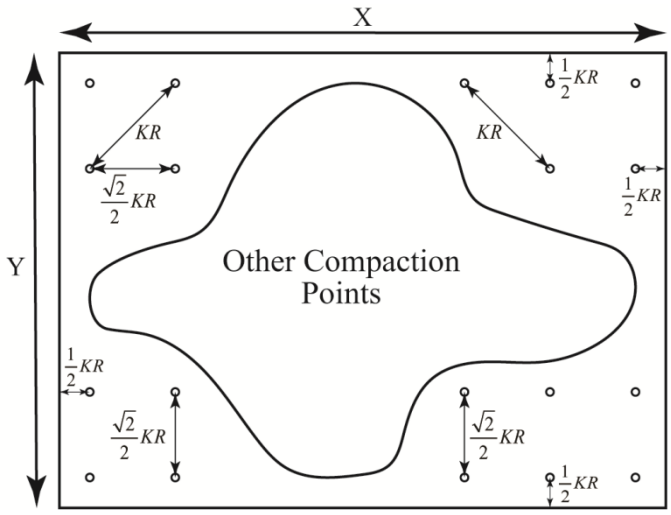

Figure 3. Square compaction pattern and the distances between tamping locations

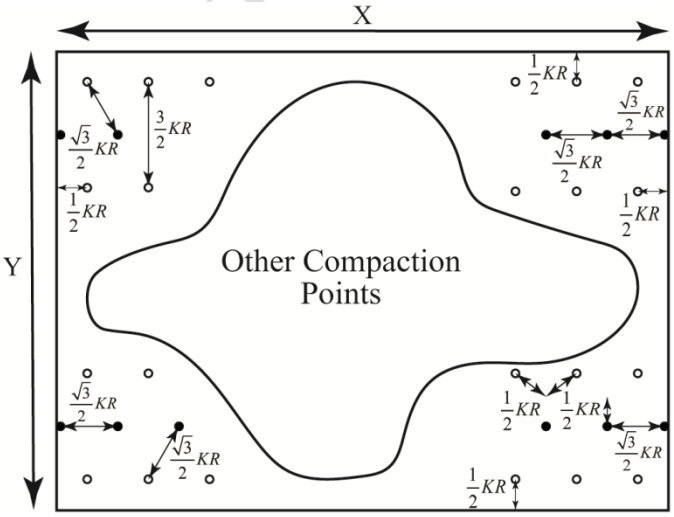

Figure 4. Diamond compaction pattern and the distances between tamping locations

The distances between tamping locations in Figures 3 and 4 were selected so that the maximum distance between adjacent tamping locations was *KR* and, as a result, required compaction was met for any point of the land along of the *X* or *Y* direction. For each square or diamond pattern case, all distances between

tamping locations were depicted. Also, the number of tamping locations inside the land was calculated according to Equations (6) and (7) for the square and diamond patterns, respectively. These numbers were required to compute the total compaction energy in each pattern. It is obvious that "NC" is a nonlinear function in terms of "R" and "K" in both cases of square or diamond patterns. Equations (6) and (7) were obtained employing Figures 3 and 4 by multiplying the number of rows and columns of tamping locations. The number of rows and columns is calculated by dividing the total length of land in any direction by distances between tamping locations. In square pattern, a distance equal to 0.5*KR* exists between tamping locations and the boundary of land. The distance value on each side should be subtracted from the total amounts of *X* or *Y* before division. In the diamond pattern, the available distance is different for hollow and solid circle signs and is indicated precisely in Figure 4. It is essential to remember that solid and hollow circle signs are the same regarding compaction properties and the distinction is just for facilitating their enumeration.

$$NC_{Square} = n_1 \times n_2 = \left(\frac{(Y - KR)}{\frac{\sqrt{2}}{2}(KR)} + 1\right) \times \left(\frac{(X - KR)}{\frac{\sqrt{2}}{2}(KR)} + 1\right) \tag{6}$$

$$NC_{Diamond} = n_1' \times n_2' + n_1'' \times n_2''$$
$$= \left(\frac{(Y - KR)}{\frac{3}{2}KR} + 1\right) \times \left(\frac{(X - KR)}{\frac{\sqrt{3}}{2}(KR)} + 1\right) + \left(\frac{(Y - 2(\frac{5}{4}KR))}{\frac{3}{2}KR} + 1\right) \times \left(\frac{(X)}{\frac{\sqrt{3}}{2}(KR)} + 1\right) \tag{7}$$

In this paper, the objective function is assumed to required energy (or cost, equivalently) of DC according to Equation (8). The decision variables in the optimization problem are tamper mass (*M*), drop height (*H*), the number of drops in each point (*N*) and the number of tamping locations in the whole land (*NC*).

$$Minimize\,(F = NC \times N \times M \times g \times H) \tag{8}$$

where *H*, *M* and *N* are forced to be integer numbers in this study according to practical applications. Value of *N* is restricted to 120 to facilitate the optimization procedure; however, there is no limitation in practical applications.

Regular constraints incorporated in optimization problems are according to Equations (9) to (15).

$$Z'' \le Z' \le Z \tag{9}$$

$$Reuired\ \ Depth\ for\ Compaction \le Z' \tag{10}$$

$$0.5m \le Z'' \le Foundation\ \ Depth \tag{11}$$

$$5tons \le M \le 40tons \tag{12}$$

$$10m \le H \le 40m \tag{13}$$

$$N \le 120 \tag{14}$$

$$1.2 \le K \le 2 \tag{15}$$

where foundation depth is the depth that the foundation is constructed and the required depth for compaction is the depth that a specified amount of compaction (ΔD_r) is required and is undoubtedly more than the foundation depth. The study driven by Oshima and Takada (1999) is one the few ones that considered the influence of "M", "N" and "H" on the dimension and degree of compaction in sandy soils. The dimensions of compacted bubbles and the degree of compaction in terms of different values of "R" and "Z" are investigated. This study was performed experimentally and the results were assumed valid for our study.

Solving the optimization problem within Equations (8) to (15) requires efficient algorithms to conquer the non-convex and non-linear nature of the problem. As a well-known metaheuristic optimization method, GA is one of the best choices. This research used Solver Add-in in Microsoft Excel package to implement GA where required parameters were adjusted before starting the solution. Objective function and constraints were defined in Solver, while the population size in each generation and other GA parameters were regulated. Population size and mutation rate were equal to 200 and 0.075, respectively. The main advantage of the GA is moving toward the global extremum in a non-convex problem. However, there is no guarantee to achieve the global extrimum, exactly. As a result, a gradient-based algorithm is required to get the GA answer as an initial guess and continue the search process. In the current study, Generalized Reduced Gradient (GRG) method available again in Solver Add-in was employed to improve the GA results. GRG gets the near-optimum answers obtained by GA and converges to exact value of global extrimum. Initial GA cooperation is essential because GRG needs help finding global extremum. Generally, gradient-based algorithms like GRG may be trapped in local extrimum without support of metaheuristic algorithms. This paper's main objectives are to examine the proposed method's effectiveness and compare the square and diamond compaction patterns. For this purpose, four square lands with dimensions of 30m, 50m, 100m and 200m were assumed, and the total required compaction energy was calculated.

Sensitivity analysis was also performed according to Equations (16) and (17) to show the influence of different parameters on the depth and radius of the compaction zone. Differentiating of *Z* and *R* in terms of *M*, *N* and *H* is performed by applying Equations (2) and (3).

$$dZ = \frac{\partial Z}{\partial M}dM + \frac{\partial Z}{\partial N}dN + \frac{\partial Z}{\partial H}dH = 0.434 b_z \left(\frac{dM}{M} + \frac{dN}{N} + \frac{dH}{2H}\right) \quad (16)$$

$$dR = \frac{\partial R}{\partial M}dM + \frac{\partial R}{\partial N}dN + \frac{\partial R}{\partial H}dH = 0.434 b_R \left(\frac{dM}{M} + \frac{dN}{N} + \frac{dH}{2H}\right) \quad (17)$$

Results and Discussion

Before considering the optimization results, it is appropriate to analyze the variation of *Z* and *R* in terms of three influential variables of *M*, *H* and *N*. This analysis specifies each variable's impact on the compacted zone's depth and radius. Figure 5 is drawn according to Equations (2) and (3) for cases ΔD_r equal to 10%, 20% or 40%. The values of a_z, b_z, a_R, b_R are based on the proposed values by Oshima and Takada (1999). As expected, the least required compaction $(\Delta D_r = 10\%)$ results in the largest amounts of *Z* and *R* and vice versa.

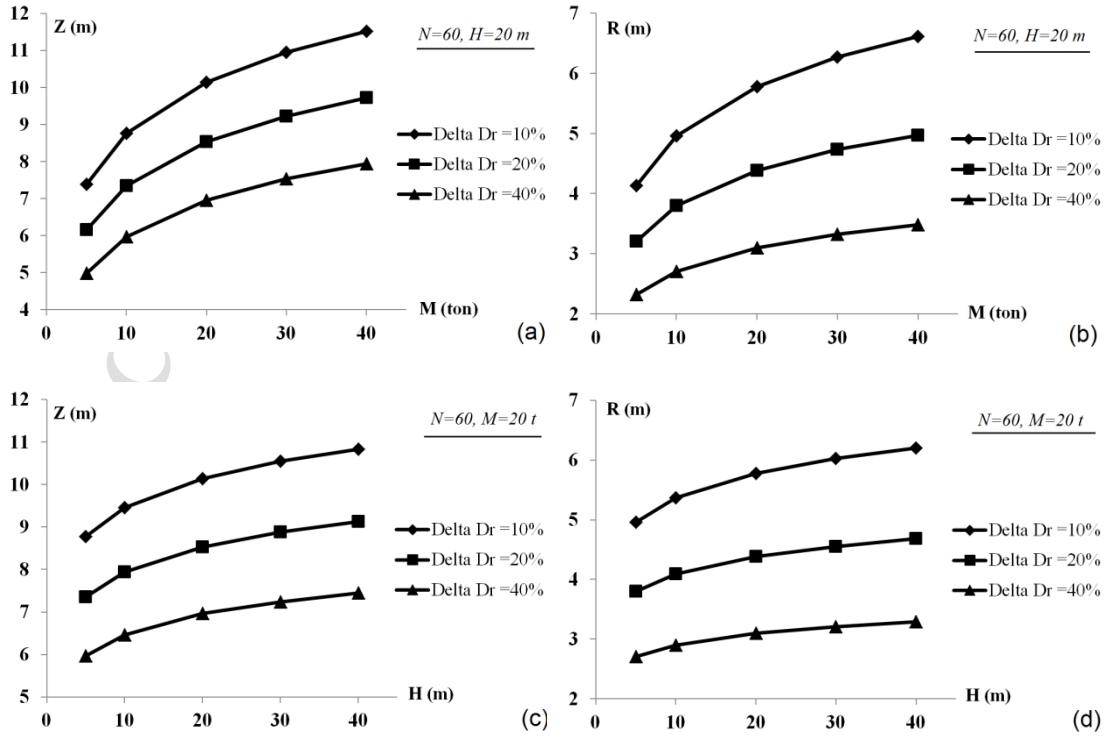

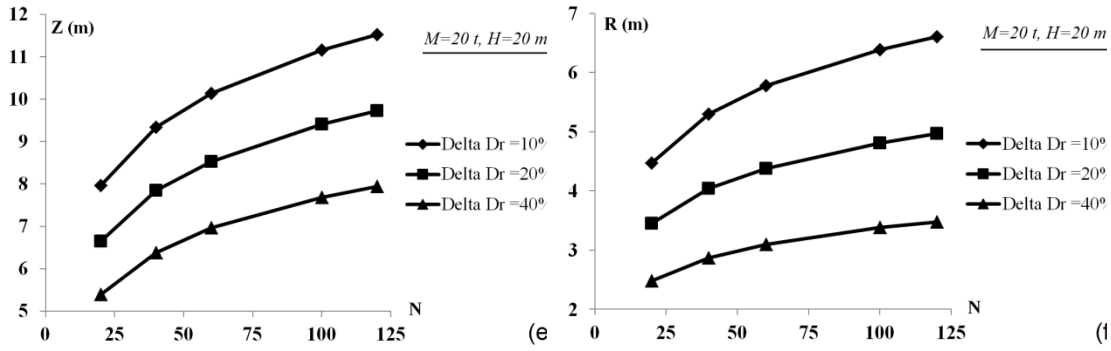

Figure 5. Variation of depth and radius of compacted zone in terms of the effective DC variables, a) *Z* vs. *M* for *N*=60 and *H*=20m, b) *R* vs. *M* for *N*=60 and *H*=20m, c) *Z* vs. *H* for *M*=20t and *N*=60, d) *R* vs. *H* for *M*=20t and *N*=60, e) *Z* vs. *N* for *M*=20t and *H*=20m and f) *R* vs. *N* for *M*=20t and *H*=20m

Figure 5 indicates that *H* has a minor influence on the depth and radius of the compaction zone when compared to other variables. This is induced regarding the relatively horizontal curves for variation of *Z* and *R* versus *H* in Figures 5(c) and 5(d) which also is concluded from the results of sensitivity analysis obtained by Equations (16) and (17). The reason is the small value for the coefficient of *dH* in Equations (16) and (17) because of the presence of "2" in the denominator of the coefficient. On the other hand, variables *M* and *N* are more effective than *H* to increase the depth and radius of compaction zone. The steep curves of *Z* and *R* versus *M* and *N* indicate the influential nature of these variables in improving the compaction zone. Considering Equations (16) and (17), it is concluded that *M* is even more effective than *N*. The reason is that usually, *dM* has a larger coefficient than *dN*. In other words, the values of *N* are normally more than *M* (in terms of tons) and thus $(1/M > 1/N)$. However, the tamper mass *M* may have some limitations to implement in practical applications.

Calculating the minimum required energy for compaction in each square and diamond pattern case and comparing them is another objective of this study. It is apparent that compaction energy is dependent on parameters like *Z′*, *Z″* and ΔD_r, where more values for parameters *Z′* or ΔD_r cause more required energy. Small value of *Z″* on the other hand needs more tamping locations and thus more energy. However, a minimal value of *Z″* may cause an infeasible situation in the solution procedure. Generally, infinite combinations of *Z′*, *Z″* and ΔD_r may occur. As a typical example, Table 1 indicates the obtained values of DC optimization for *Z′=6*, *Z″=2* and ΔD_r*=40%*. The results show that the preferred value for *M* is the maximum practical (40 tons here). The optimum value for *N* is also the maximum assumed value in the

problem. However, in some cases, the value for *N* has a slight deviation from the maximum. It seems it is taking place because only integer values for *M*, *N* and *H* are allowed. The optimum values of *M* and *N* are the maximum allowed ones because of the larger coefficients of *dM and dN* to improve *dZ* and *dR* in Equations (16) and (17).

Another important point regarding Table 1 is the efficiency of the diamond pattern compared with square one. Results indicate that ratio of the required energy of diamond to the square pattern is between 0.75 and 0.9; however, no regular trend is observed in terms of land dimension. It seems that the diamond pattern is more effective than the square one due to better interlock of compaction bubbles in each other.

The proposed approach in this study is quite analytical and is performed based on the empirical equations obtained by Oshima and Takada (1999). As a result, the verification phase has no sense here, and optimization results are valid for all cases.

Table 1. Obtained DC variables for various land dimensions for *Z'=6, Z''=2* and ΔD_r*=40%*

Land Dimension (m × m)		30×30	50×50	100×100	200×200
square pattern for DC	*K*	1.483	1.476	1.448	1.455
	N	120	119	120	117
	H(m)	19	19	18	19
	M(ton)	40	40	40	40
	F(MJ)	32197	107316	488042	2093690
diamond pattern for DC	*K*	1.469	1.429	1.487	1.467
	N	118	119	120	118
	H(m)	19	18	19	19
	M(ton)	40	40	40	40
	F(MJ)	25504	96627	374740	1602377

Conclusion

This paper presents an innovative method to implement dynamic compaction so that minimum compaction energy is consumed while required constraints are satisfied. For this purpose the DC problem is formulated regarding all physical and practical constraints. The depth and radius of the compacted zone are estimated for a single tamper. Then, extra equations are developed to determine the intersection points of compaction bubbles. Afterwards, the best values for horizontal distances between tamping locations are determined to satisfy compaction requirements specified by the operator. Obtaining the best horizontal distances needs to

solve a non-linear and non-convex optimization problem. Generally, finding the global optimum in a non-convex problem is a challenge. To overcome this challenge, a combination of metaheuristic (GA) and gradient-based (GRG) algorithms was employed. All calculations are performed for two compaction patterns of square and diamond. A sensitivity analysis is also performed to identify the impacts of influential variables on the DC procedure. The impacts of variables are compared and some discussion about the range of each one is presented. Finally, the main obtained points are as follows:

Tamper mass (*M*), drop height (*H*) and the number of drops in each tamping location (*N*) affect the radius and depth of the compacted zone. The compaction energy is enhanced by increasing each of these variables. However, the tamper mass and the number of drops in each tamping location are the most effective variables for increasing the radius and depth of compacted zone while the drop height is the least effective one. It is required to note that tamper mass and drop height have some practical limitations, while the number of drops has no such limitation. The required energy (or equivalently cost) for DC in a diamond pattern is about 75% to 90% of the energy of a square pattern, for the same conditions of compaction. Applying the following results may benefit operators economically during DC, especially in large projects.

- The optimum value for *K* is between 1.4 and 1.5 in all cases.
- The optimum value for *M* is the largest practical value in all cases.
- The optimum value for *N* is the largest allowable value. However, in some cases the maximum values of *N* are not obtained due to the integer variables incorporated in the problem.
- The optimum value for *H* is about 18m to 19m for DC operations with dimensions near to the values of this study. This value is almost half of the maximum allowed value for *H*. It seems the reason is the presence of number "2" in the denominator of the coefficient of *dH* within sensitivity analysis equations.

References

Adam, D., Brandl, H., Kopf, F., Paulmichl, I. (2007). "Heavy tamping integrated dynamic compaction control", *Ground Improvement*, *11*(4), 237–243. https://doi.org/10.1680/grim.2007.11.4.237

An, Z., Liu, T., Zhang, Z., Zhang, Q., Huangfu, Z., Li, Q. (2020). "Dynamic optimization of compaction process for rockfill materials", *Automation in Construction*, *110* (2020). https://doi.org/10.1016/j.autcon.2019.103038

Anand, A. and Sarkar, R. (2021). "A comprehensive study on bearing behavior of cement–fly ash composites through experimental and probabilistic investigations", *Innovative Infrastructure Solutions*, *6*(1). https://doi.org/10.1007/s41062-020-00404-w

Arslan, H., Baykal, G., Ertas, O. (2009). "Discussion: Influence of tamper weight shape on dynamic compaction", *Proceedings of the Institution of Civil Engineers: Ground Improvement*, *162*(3), 153–154. https://doi.org/10.1680/grim.2009.162.3.153

Bağrıaçık, B., Yıldırım, Z. B., Güner, E. D., Beycioğlu, A. (2020). "Assessment of pipe powder in soil improvement applications: an optimization by response surface methodology", *Arabian Journal of Geosciences*, *13*(19), 1–11. https://doi.org/10.1007/s12517-020-05962-y

Biabani, F., Razzazi, A., Shojaee, S., Hamzehei-Javaran, S. (2022). "DESIGN AND APPLICATION OF A HYBRID META-HEURISTIC OPTIMIZATION ALGORITHM BASED ON THE COMBINATION OF PSO, GSA, GWO AND CELLULAR AUTOMATION", *Iran University of Science & Technology*, *12*(3), 279–312. http://ijoce.iust.ac.ir/article-1-520-en.html

Chen, L., Qiao, L., Li, Q. (2019). "Study on dynamic compaction characteristics of gravelly soils with crushing effect", *Soil Dynamics and Earthquake Engineering*, *120*(January 2017), 158–169. https://doi.org/10.1016/j.soildyn.2019.01.034

Chow, Y. K., Yong, D. M., Yong, K. Y., Lee, S. L. (1992). "Dynamic compaction analysis", *Journal of Geotechnical Engineering*, *118*(8), 1141–1157. https://doi.org/10.1061/(ASCE)0733-9410(1992)118:8(1141)

Du, J., Wu, S., Hou, S., Wei, Y. (2019). "Deformation Analysis of Granular Soils under Dynamic Compaction Based on Stochastic Medium Theory", *Mathematical Problems in Engineering*, *2019*. https://doi.org/10.1155/2019/6076013

Fazli, H. (2022). "AN EFFICIENT METHOD FOR OPTIMUM PERFORMANCE-BASED SEISMIC DESIGN OF FUSED BUILDING STRUCTURES", *Iran University of Science & Technology*, *12*(4), 501–516. http://ijoce.iust.ac.ir/article-1-531-en.html

Feng, S. J., Du, F. L., Chen, H. X., Mao, J. Z. (2017). "Centrifuge modeling of preloading consolidation and dynamic compaction in treating dredged soil", *Engineering Geology*, *226*, 161–171. https://doi.org/10.1016/j.enggeo.2017.06.005

Feng, S. J., Du, F. L., Shi, Z. M., Shui, W. H., Tan, K. (2015). "Field study on the reinforcement of collapsible loess using dynamic compaction", *Engineering Geology*, *185*, 105–115.

https://doi.org/10.1016/j.enggeo.2014.12.006

Feng, S. J., Shui, W. H., Gao, L. Y., He, L. J., Tan, K. (2010). "Field studies of the effectiveness of dynamic compaction in coastal reclamation areas", *Bulletin of Engineering Geology and the Environment*, *69*(1), 129–136. https://doi.org/10.1007/s10064-009-0242-x

Feng, S. J., Tan, K., Shui, W. H., Zhang, Y. (2013). "Densification of desert sands by high energy dynamic compaction", *Engineering Geology*, *157*, 48–54. https://doi.org/10.1016/j.enggeo.2013.01.017

Feng, T. W., Chen, K. H., Su, Y. T., Shi, Y. C. (2000). "Laboratory investigation of effiency of conical-based pounders for dynamic compaction", *Geotechnique*, *50*(6), 667–674. https://doi.org/10.1680/geot.2000.50.6.667

Ghanbari, M., and Bayat, M. (2022). "Effectiveness of Reusing Steel Slag Powder and Polypropylene Fiber on the Enhanced Mechanical Characteristics of Cement-Stabilized Sand", *Civil Engineering Infrastructures Journal*, *55*(2), 47–63. https://doi.org/10.22059/CEIJ.2021.319310.1742

Ghassemi, A., Pak, A., Shahir, H. (2010). "Numerical study of the coupled hydro-mechanical effects in dynamic compaction of saturated granular soils", *Computers and Geotechnics*, *37*(1–2), 10–24. https://doi.org/10.1016/j.compgeo.2009.06.009

Ghassemi, A., and Shahebrahimi, S. S. (2020). "Discrete Element Modeling of Dynamic Compaction with Different Tamping Condition", *Civil Engineering Infrastructures Journal*, *53*(1), 173–188.

Goldberg, D. E. (1989). *Genetic algorithms in search, optimization, and machine learning*, Addison-Wesley Professional. United States.

Gu, Q., Lee, F. H. (2002). "Ground response to dynamic compaction of dry sand", *Geotechnique*, *52*(7), 481–493. https://doi.org/10.1680/geot.2002.52.7.481

Haghbin, M., and Ghazavi, M. (2016). "Seismic Bearing Capacity of Strip Footings on Pile-Stabilized Slopes", *Civil Engineering Infrastructures Journal*, *49*(1), 111–126. https://doi.org/10.7508/ceij.2016.01.008

Holland, J. H. (1992). *Adaptation in Natural and Artificial Systems.* MIT Press. United States.

Hosseini, P., Kaveh, A., Hoseini Vaez, S. R. (2022). "ROBUST DESIGN OPTIMIZATION OF SPACE TRUSS STRUCTURES", *Iran University of Science & Technology*, *12*(4), 595–608. http://ijoce.iust.ac.ir/article-1-536-en.html

Hu, R. L., Yeung, M. R., Lee, C. F., Wang, S. J. (2001). "Mechanical behavior and microstructural

variation of loess under dynamic compaction", *Engineering Geology*, *59*(3–4), 203–217. https://doi.org/10.1016/S0013-7952(00)00074-0

Kalantary, F. and Kahani, M. (2019). "Optimization of the biological soil improvement procedure", *International Journal of Environmental Science and Technology*, *16*(8), 4231–4240. https://doi.org/10.1007/s13762-018-1821-9

Kaveh, A. and Zaerreza, A. (2022). "OPTIMUM DESIGN OF THE BRACED DOME WITH FREQUENCY CONSTRAINT USING THE IMPROVED SHUFFLED BASED JAYA ALGORITHM", *Iran University of Science & Technology*, *12*(4), 609–625. http://ijoce.iust.ac.ir/article-1-537-en.html

Li, W., Gu, Q., Su, L., Yang, B. (2011). "Finite element analysis of dynamic compaction in soft foundation", *Procedia Engineering*, *12*, 224–228. https://doi.org/10.1016/j.proeng.2011.05.035

Mehdipour, S. and Hamidi, A. (2017). "Impact of Tamper Shape on the Efficiency and Vibrations Induced During Dynamic Compaction of Dry Sands by 3D Finite Element Modeling", *Civil Engineering Infrastructures Journal*, *50*(1), 151–163. https://doi.org/10.7508/ceij.2017.01.009

Ménard, L. and Broise, Y. (1975). "Theoretical and Practical Aspect of Dynamic Consolidation", *Geotechnique*, *25*(1), 3–18. https://doi.org/10.1680/geot.1975.25.1.3

Mostafa, K. F. and Liang, R. Y. (2011). "Numerical Modeling of Dynamic Compaction in Cohesive Soils", *Geotechnical Special Publication*, *2011*, 738–747. https://doi.org/10.1061/41165(397)76

Oshima, A. and Takada, N. (1999). "Evaluation compacted area of heavy damping by cone point resistance", *In: Proceedings of the Centrifuge*, *Tokyo*, 1641–1644.

Paranthaman, R. and Azam, S. (2022). "Effect of compaction on desiccation and consolidation behavior of clay tills", *Innovative Infrastructure Solutions*, *7*(1), 1–8. https://doi.org/10.1007/s41062-021-00644-4

Pasdarpour, M., Ghazavi, M., Teshnehlab, M., Sadrnejad, S. A. (2009). "Optimal design of soil dynamic compaction using genetic algorithm and fuzzy system", *Soil Dynamics and Earthquake Engineering*, *29*(7), 1103–1112. https://doi.org/10.1016/j.soildyn.2008.09.003

Raja, P. S. K. and Thyagaraj, T. (2020). "Effect of compaction time delay on compaction and strength behavior of lime-treated expansive soil contacted with sulfate", *Innovative Infrastructure Solutions*, *5*(1), 1–15. https://doi.org/10.1007/s41062-020-0268-2

Sahlabadi, S. H., Bayat, M., Mousivand, M., Saadat, M. (2021). "Freeze–Thaw Durability of Cement-

Stabilized Soil Reinforced with Polypropylene/Basalt Fibers", *Journal of Materials in Civil Engineering*, *33*(9), 04021232. https://doi.org/10.1061/(asce)mt.1943-5533.0003905

Salehi, M., Bayat, M., Saadat, M., Nasri, M. (2021). "Experimental Study on Mechanical Properties of Cement-Stabilized Soil Blended with Crushed Stone Waste", *KSCE Journal of Civil Engineering*, *25*(6), 1974–1984. https://doi.org/10.1007/s12205-021-0953-5

Scott, B., Jaksa, M., Mitchell, P. (2021). "Depth of influence of rolling dynamic compaction", *Proceedings of the Institution of Civil Engineers: Ground Improvement*, *174*(2), 85–94. https://doi.org/10.1680/jgrim.18.00117

Shen, M., Martin, J. R., Ku, C. S., Lu, Y. C. (2018). "A case study of the effect of dynamic compaction on liquefaction of reclaimed ground", *Engineering Geology*, *240*, 48–61. https://doi.org/10.1016/j.enggeo.2018.04.003

Silveira, I. A. and Rodrigues, R. A. (2020). "Collapsible Behavior of Lateritic Soil Due to Compacting Conditions", *International Journal of Civil Engineering*, *18*(10), 1157–1166. https://doi.org/10.1007/s40999-020-00523-6

Wang, H. L. and Yin, Z. Y. (2020). "High performance prediction of soil compaction parameters using multi expression programming", *Engineering Geology*, *276*, 105758. https://doi.org/10.1016/j.enggeo.2020.105758

Wang, S. Y., Chan, D. H., Lam, K. C., Au, S. K. A. (2013). "A new laboratory apparatus for studying dynamic compaction grouting into granular soils", *Soils and Foundations*, *53*(3), 462–468. https://doi.org/10.1016/j.sandf.2013.04.007

Wang, Y., Li, X. B., Jiang, W. D. (2003). "Application of fuzzy model of multi-objective system to optimization of parameters of dynamic compaction", *Rock and Soil Mechanics-Wuhan*, *24*(3), 410–412.

Wu, S., Wei, Y., Zhang, Y., Cai, H., Du, J., Wang, D., Yan, J., Xiao, J. (2020). "Dynamic compaction of a thick soil-stone fill: Dynamic response and strengthening mechanisms", *Soil Dynamics and Earthquake Engineering*, *129*(November 2019). https://doi.org/10.1016/j.soildyn.2019.105944

Zhang, R., Sun, Y., Song, E. (2019). "Simulation of dynamic compaction and analysis of its efficiency with the material point method", *Computers and Geotechnics*, *116*(August). https://doi.org/10.1016/j.compgeo.2019.103218

Zou, J. F., Luo, H., Yang, X. L. (2008). "Effective depth of dynamic compaction in embankment built

with soils and rocks", *Journal of Central South University of Technology (English Edition)*, *15*(SUPPL. 2), 34–37. https://doi.org/10.1007/s11771-008-0432-x